Histochem Cell Biol (2005) 123: 217–228
DOI 10.1007/s00418-005-0752-y

REVIEW

Sabine M. Görisch · Peter Lichter · Karsten Rippe

Mobility of multi-subunit complexes in the nucleus: accessibility and dynamics of chromatin subcompartments

Accepted: 15 December 2004 / Published online: 14 April 2005

Abstract The cell nucleus contains a number of mobile subnuclear organelles involved in RNA processing, transcriptional regulation and antiviral defence like Cajal and promyelocytic leukaemia (PML) bodies. It remains an open question how these bodies translocate to specific nuclear regions within the nucleus to exert their biological function. The mobility and localisation of macromolecules in the nucleus are closely related to the dynamic organisation and accessibility of chromatin. This relation has been studied with biologically inert fluorescent particles like dextrans, polystyrene nanospheres and inactive protein crystals formed by the Mx1-YFP fusion protein or other ectopically expressed proteins like vimentin. As reviewed here, properties of the chromatin environment can be identified from these experiments that determine the mobility of Cajal and PML bodies and other supramolecular complexes.

Abbreviation D: Diffusion coefficient · FISH: Fluorescence in situ hybridisation · ICD: Interchromosomal domain · MSD: Mean square displacement · NLS: Nuclear localisation sequence · PML: Promyelocytic leukaemia · SPT: Single particle tracking

S. M. Görisch (✉) · P. Lichter
Division of Molecular Genetics,
Deutsches Krebsforschungszentrum,
Im Neuenheimer Feld 280, 69120
Heidelberg, Germany
E-mail: goerisch@mdc-berlin.de
Tel.: +49-30-94172260
Fax: +49-30-94172336

Present address: S. M. Görisch
Max Delbrück Center for Molecular Medicine,
13125 Berlin, Germany

K. Rippe
AG Molekulare Biophysik,
Kirchhoff-Institut für Physik,
Im Neuenheimer Feld 227,
69120 Heidelberg, Germany

Chromatin organisation in the nucleus

The nuclear envelope confines the cell nucleus and separates the genome and the factors needed for replication and transcription in the nucleoplasm from the cytoplasm. The nucleoplasm is further compartmentalised into a number of subnuclear organelles, in which certain protein and nucleic acid components with specific biological activities are concentrated. The most prominent example is the nucleolus, which contains regions with ribosomal RNA genes from several chromosomes, and also contains the machinery for the assembly of ribosomal subunits. Other nuclear substructures include the SC35 domains (“Speckles”), Cajal and promyelocytic leukaemia (PML) bodies (Spector 2001; Gall 2003; Lamond and Sleeman 2003; Lamond and Spector 2003; Spector 2003). The localisation, organisation, dynamics and biological activities of these suborganelles appear to be closely related to gene expression and are, therefore, an important subject of current research.

Using whole chromosome painting probes and fluorescence in situ hybridisation (FISH), a territorial organisation of interphase chromosomes has been demonstrated (Lichter et al. 1988; Pinkel et al. 1988; Cremer et al. 1993). Chromosome territories have irregular shapes and occupy discrete nuclear positions with little overlap (Fig. 1). In general, gene-rich chromosomes are located more in the nuclear interior while gene-poor chromosome territories are located at the nuclear periphery (Croft et al. 1999; Boyle et al. 2001; Cremer et al. 2001; Tanabe et al. 2002; Dietzel et al. 2004). In agreement with this, non-transcribed sequences were predominantly found at the nuclear periphery or perinucleolar while active genes and gene-rich regions tended to localise on chromosome surfaces exposed to the nuclear interior or on loops extending from the territories (Kurz et al. 1996; Dietzel et al. 1999; Volpi et al. 2000; Mahy et al. 2002; Scheuermann et al. 2004).

Promyelocytic leukaemia and Cajal bodies are preferably located outside of chromosome territories (Zirbel

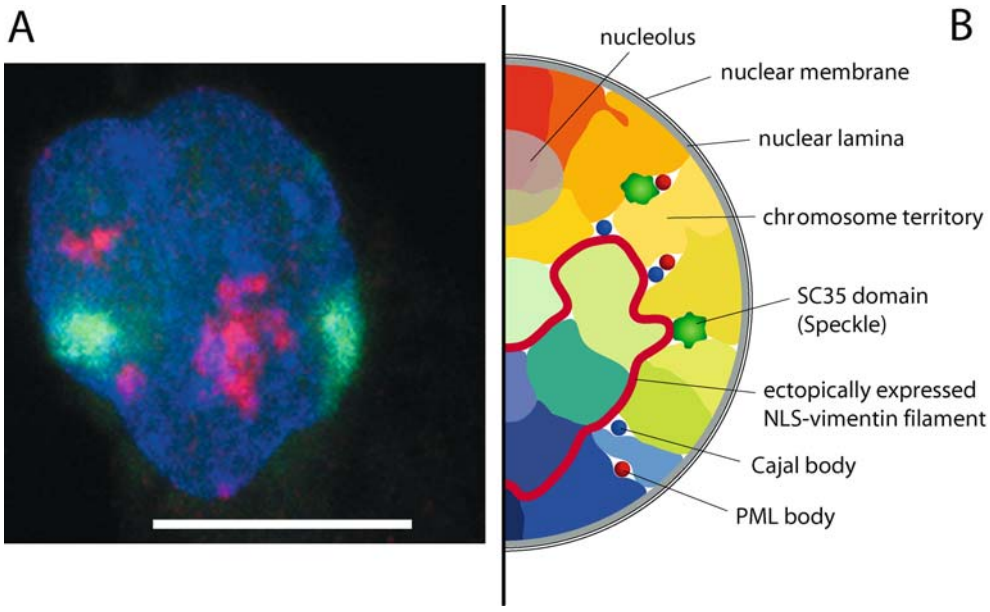

Fig. 1 Nuclear organisation. **a** U2OS cell nucleus DAPI counterstained with FISH-painted chromosome territories 3 (*green*) and 18 (*red*). Scale bar represents 10 μm. Image courtesy of S. Geiger; DKFZ Heidelberg. **b** Schematic illustration of the compartmentalisation of an interphase nucleus showing nuclear bodies, Speckles and NLS-vimentin located outside of chromosome territories

et al. 1993; Bridger et al. 1998). In addition, specific RNA transcripts are found in track-like or spherical accumulations within the nucleus (Lawrence et al. 1989; Xing et al. 1993; Lampel et al. 1997; Bridger et al. 2005). Nuclear spaces accessible to large supramolecular complexes were examined with vimentin modified to carry a nuclear localisation sequence (NLS) as well as nuclear crystalline Mx1-YFP particles. NLS-vimentin and Mx1-YFP were both found in the vicinity of nuclear bodies (Bridger et al. 1998; Görisch et al. 2004) (Fig. 2a, b) and also next to each other (Richter et al. 2005) (Fig. 2c, d). NLS-vimentin was predominantly located outside of FISH-labelled chromosome territories (Bridger et al. 1998), and similar results were observed for NLS-vimentin and Mx1-YFP in BrdU-labelled cells (Fig. 2e, f). These experimental findings support the concept of a functional nuclear space, the interchromosomal domain (ICD) compartment (Cremer et al. 1993; Zirbel et al. 1993; Herrmann and Lichter 1999). According to the ICD model, the interface between chromosome territories is more easily accessible to large nuclear complexes than regions within the territory (Fig. 1b) (reviewed in Cremer and Cremer 2001). More recently, it has been proposed that chromosome territories are further organised into 1-Mb domains (Zink et al. 1999; Berezney et al. 2000; Visser et al. 2000; Cremer and Cremer 2001; Cremer et al. 2004; Kreth et al. 2004), extending the more accessible space to open intra-chromosomal regions surrounded by denser chromatin domains. Using high-resolution light microscopy, an apparent bead-like structure of chromatin can be visualised in which ~1-Mb domains of chromatin are more densely packed into an approximately spherical subcompartment structure with dimensions of 300–400 nm (Müller et al. 2004). As indicated in Fig. 3, these domains are thought to be formed by a specific folding of the 30-nm chromatin fibre, to which the chain of nucleosomes associates under physiological salt concentrations (Woodcock and Dimitrov 2001; Hansen 2002; Adkins et al. 2004). However, the resolution of the light microscope is not sufficient to identify the organisation of the 30-nm chromatin fibre that leads to dense chromatin regions and the formation of the ~1-Mb domains. The different models that have been proposed are shown in Fig. 3: The radial-loop models propose small loops of roughly 100 kb arranged in rosettes (Hamkalo and Rattner 1980; Pienta and Coffey 1984; Münkel et al. 1999; Paul and Ferl 1999) (Figure 3a) while the random-walk/giant-loop (RW/GL) model proposes large loops of chromatin back-folded to an underlying structure (Sachs et al. 1995) (Fig.3b). In the chromonema model (Sedat and Manuelidis 1978; Belmont and Bruce 1994; Tumbar et al. 1999), the compaction of the 30-nm fibre is achieved by its folding into 60- to 80-nm fibres that undergo additional folding to 100- to 130-nm chromonema fibres (Figure 3c).

The local variations of the chromatin density in the interphase nucleus are apparent when staining the DNA with fluorescent dyes like DAPI and Hoechst 33258 or labelling of the chromatin by incorporation of fluorescent histones (reviewed in Cremer and Cremer 2001). Nucleosome concentrations from 10 μM to 250 μM with an average value of 140 μM have been measured in the HeLa nucleus (Weidemann et al. 2003). Besides the chromatin density variations on a length scale of several hundred nanometers that have been assigned to the existence of the above-mentioned 1-Mb domains, regions in the micrometre-length scale at the nuclear periphery around the nucleolus and at the centromeres also display a high degree of compaction. These dense chromatin regions are often referred to as heterochromatin as opposed to the less dense euchromatin (reviewed in Dillon and Festenstein 2002; Dillon 2004). Heterochromatin was originally characterised by its intense staining in light microscopy images (Heitz 1928) and tight coiling observed in electron micrographs

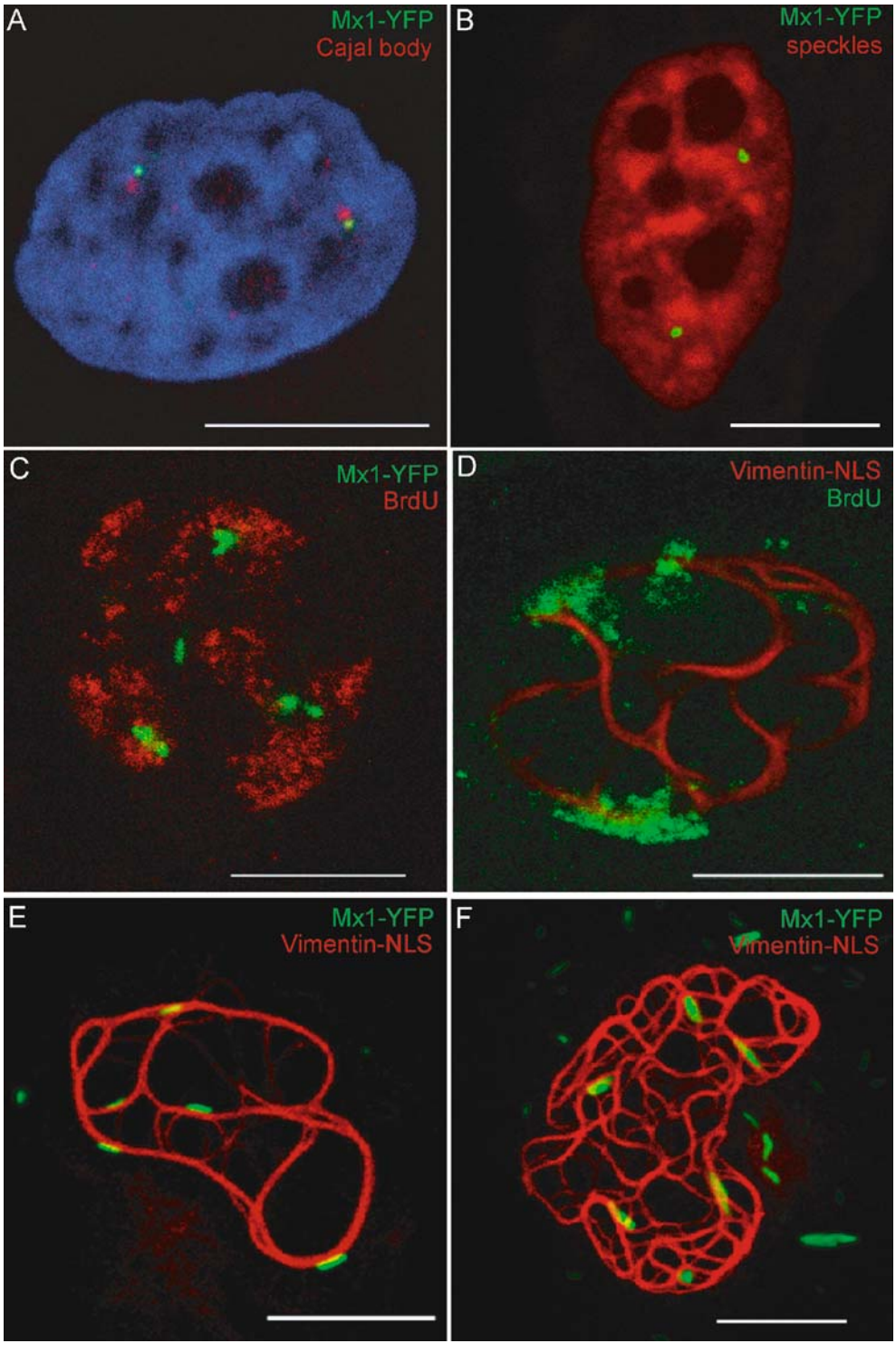

Fig. 2 A common nuclear compartment is shared by ectopically expressed proteins and nuclear bodies. Crystalline Mx1-YFP particles are located next to **a** Cajal bodies and **b** nuclear Speckles. Within this compartment other ectopically expressed proteins are also localised, as shown for Mx1-YFP and *Xenopus laevis* NLS-vimentin at **c** moderate and **d** high expression levels of *Xenopus* NLS-vimentin. These proteins are localised to regions with low chromatin density, namely, outside of chromosome territories or in intra-chromosomal openings, as demonstrated with BrdU-labelled chromosome territories for **e** Mx1-YFP particles and **f** human NLS-vimentin. Confocal sections of HeLa cells (**a** –**d**) and MCF7 cells (**e**, **f**). Scale bars represent 10 μm

(Davies 1967). It has been described as containing increased DNA methylation at cytosines, specific histone modification patterns like methylation of lysine 9 on histone H3 and histone hypoacetylation, binding of heterochromatin protein 1 (HP1), interaction with non-coding RNA and activities of the RNAi-mediated silencing machinery (Bannister et al. 2001; Lachner et al. 2001; Chadwick and Willard 2003; Hall and Lawrence 2003; Fejes Tóth et al. 2004; Grewal and Rice 2004; Maison and Almouzni 2004). Regions of so-called facultative heterochromatin are known, which display a transition from a more open transcriptionally active conformation into a biologically inactive conformation (Dillon and Festenstein 2002; Dillon 2004). The most prominent example of facultative heterochromatin is the inactivation of one of the two X chromosomes in mammalian females, which shows a strong chromatin compaction during embryogenesis into a dense structure

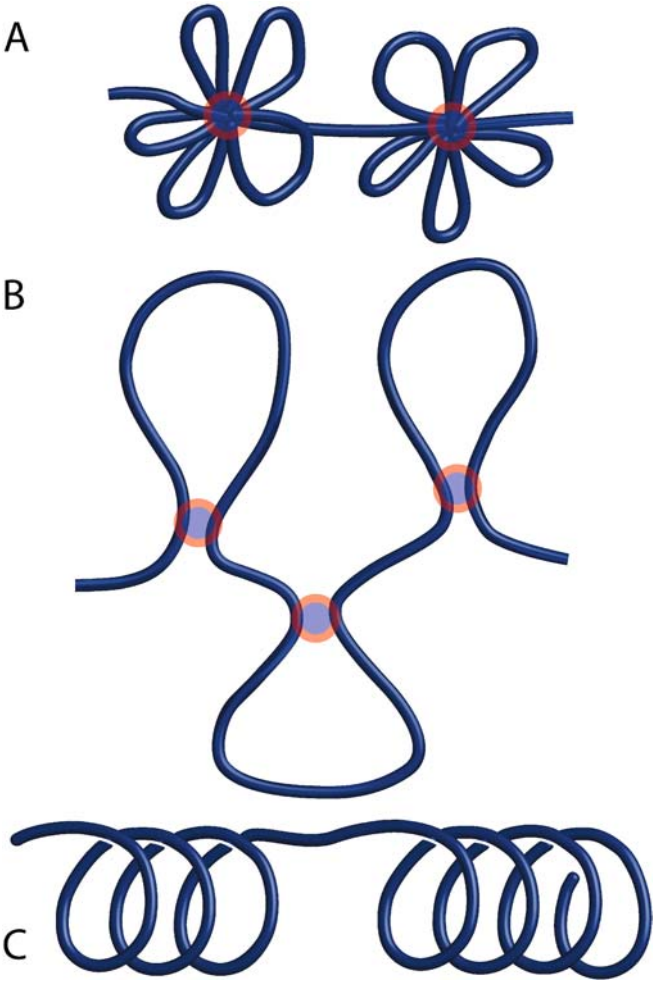

Fig. 3 Hypothetical models for the folding of the chromatin fibre during interphase, leading to the formation of 1-Mb chromatin domains. **a** the radial-loop model, **b** the random-walk/giant-loop (RW/GL) model or **c** the chromonema model

referred to as the Barr body (Chadwick and Willard 2003; Hall and Lawrence 2003; Dillon 2004). The relation of a dense heterochromatic state with a biologically inactive chromatin conformation has led to the concept that the biological activity of chromatin is regulated via its accessibility to protein factors (reviewed in Dillon and Festenstein 2002).

Size-dependent accessibility of chromatin

Depending on the degree of compaction, chromatin regions have different accessibilities. This has been visualised by progressive exclusion of microinjected and fluorescently labelled dextrans with increasing size from 4 kDa to 2.5 MDa (Fig. 4) (Görisch et al. 2003; Verschure et al. 2003). Dextrans are polymers that adopt a dynamic random-coil conformation. The size of such a particle can be described by its radius of gyration R_G (Seksek et al. 1997; Lukacs et al. 2000), which characterises the average distance of atoms from the centre of mass of the molecule. The corresponding diameter ($2\times R_G$) serves as an estimate for the minimal extensions of open regions to which the molecule has access (Lénárt et al. 2003). Approximating that the R_G value of a random coil is equivalent to the radius r of a much more rigid spherical protein, a corresponding protein molecular weight M can be calculated according to Eq. 1.

$$M = \frac{4}{3}\pi r^3 \frac{N_A}{\bar{v}} \quad (1)$$

The average value of the partial specific protein volume is $\bar{v} = 0.73$ ml g^{-1} (Durchschlag 1986) and N_A is the Avogadro number 6.022×10^{23} mol^{-1}. Up to a size of ~70 kDa (R_G~11 nm (Seksek et al. 1997)), a mostly unlimited nuclear access for dextrans has been found (Görisch et al. 2003; Verschure et al. 2003), i.e. the dextrans are homogenously distributed. According to Eq. 1, this would correspond to a molecular weight of $M = 4.6$ MDa for a spherical protein complex, suggesting that within the resolution of the light microscope (~250 nm lateral), all chromatin regions are accessible to even very large protein complexes. In agreement with this estimate, it has been shown that GFP ($M = 27$ kDa) (Wachsmuth et al. 2000) and the RNA polymerase II complex ($M = 600$ kDa) (Verschure et al. 2003) are homogenously distributed throughout the nucleus. At a dextran size of ~150 kDa, nuclear access becomes increasingly restricted. Dextrans of ~500 kDa are clearly excluded from putative heterochromatic regions while the 2.5 MDa FITC dextrans are excluded from chromatin in general and are confined to nuclear regions referred to as dextran patches (Görisch et al. 2003). These observations are in agreement with a diffusion analysis where FITC dextran particles up to 580 kDa are still mobile within the nucleoplasm whereas 2 MDa FITC-dextran particles are essentially immobile (Lukacs et al. 2000). Upon temperature shifts, no change in this behaviour can be measured (Braga et al. 2004).

It can be estimated that the average spacing of the 30-nm chromatin fibre for a nucleosome concentration in the nucleus of ~100 μM is around 100 nm; i.e. would allow the passage of complexes up to a size of ~70 nm. Even the dense chromatin regions, where a nucleosome concentration of ~260 μM has been measured, would still be accessible to particles of ~30 nm (Weidemann et al. 2003). Indeed, an exclusion from dense chromatin regions has been observed for FITC dextrans of ~150 kDa (Görisch et al. 2003), which corresponds to a size of ≥30 nm (Seksek et al. 1997). The nuclear accessibility is not only dependent on the size of the particle but will also reflect interactions with nuclear structures. This is apparent from the analysis of the effect of negative charges on the dextran distribution. While small anionic dextrans are distributed like non-charged dextrans, large anionic dextrans of 500 kDa are concentrated in nuclear foci and almost completely excluded

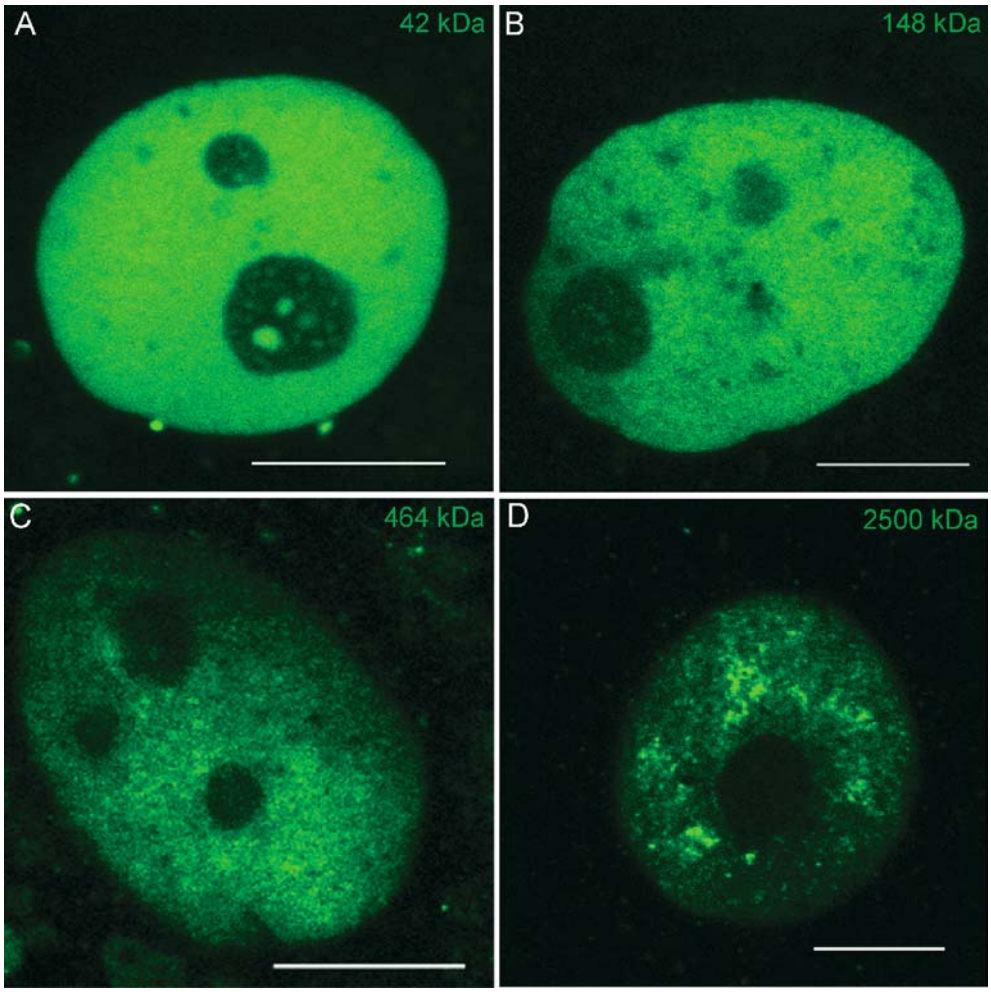

Fig. 4 Nuclear accessibility can be examined by an increase in granularity and accumulation of microinjected FITC dextrans with increasing size in HeLa cells: **a** 42 kDa, **b** 148 kDa, **c** 464 kDa and **d** 2.5 MDa FITC-dextrans. Scale bars represent 10 μm

from chromatin in contrast to non-charged dextrans of the same size (Görisch et al. 2003).

Diffusion of large particles in the nucleus

The mobility of protein complexes can be studied by a number of techniques, including FRAP (fluorescence recovery after photobleaching) and fluorescence correlation spectroscopy (FCS) (Bastiaens and Pepperkok 2000; Lippincott-Schwartz et al. 2001), e.g. the RNA polymerase II (Kimura et al. 2002) or the above-mentioned GFP (Wachsmuth et al. 2000). For larger particles that can be detected in the light microscope, the mobility is analysed by methods of single particle tracking (SPT) in which a time series of images is collected to determine the movement of the particle over time (Qian et al. 1991). In these experiments, nuclear particles usually displayed no directed movements in the nucleus. In addition, the observed accessibility and mobility of the particles are size-dependent and frequently reflect features of the chromatin environment. Furthermore, the apparent speed with which a particle translocates from its start position depends on the observation time if the velocity of the movement is defined as the distance travelled by the body divided by the corresponding time period. A more useful parameter to describe this random movement, independent of the observation time, is the diffusion coefficient D of the particle. This parameter is determined from the mean square displacement (MSD) or $< d^2 >$ a molecule travels in a given time period Δt. It is computed on a time series of fluorescence images after corrections for any movements of the whole cell (Bacher et al. 2004; Rieger et al. 2004), according to Eq. 2.

$$\mathrm{MSD} = \left\langle \mathrm{d}^2(\Delta t) \right\rangle = \left\langle [\mathrm{d}(t) - \mathrm{d}(t + \Delta t)]^2 \right\rangle \tag{2}$$

The squared distance d^2 between the two positions $\mathrm{d}(t)$ and $\mathrm{d}(t + \Delta t)$ of the particle before and after a time Δt is measured, averaged for all identical values of Δt and then plotted against time Δt. For a diffusion process in n dimensions according to Eq. 3 it is

$$\mathrm{MSD} = \left\langle \mathrm{d}^2(\Delta t) \right\rangle = 2n\,\Gamma\,\Delta t^{\alpha} \tag{3}$$

with Γ being a generalised transport coefficient, which for a value of $\alpha = 1$ equals the diffusion coefficient D. In

this case, a plot of MSD versus time will yield a straight line with a slope of $2nD$. It is noted that for an isotropic movement of the particle in three dimensions ($n=3$), the value determined for D from projections to two dimensions ($n=2$) will be the same as that obtained from the analysis of 3D data sets, as shown, for example, in the supplementary material of reference (Görisch et al. 2004). For $\alpha \neq 1$, an apparent time dependence of the diffusion coefficient is observed, as the slope of the MSD versus Δt plot is no longer constant and one speaks of "anomalous diffusion". These deviations of the mobility from that of free diffusion can be further distinguished as confined diffusion, obstructed diffusion or directed motion (Sako and Kusumi 1994; Simson et al. 1998; Wachsmuth et al. 2000; Görisch et al. 2004) (Fig.5). Using a logarithmic plot of the MSD versus time relationship, a graphic test for anomalous diffusion can be conducted (Saxton 1994; Platani et al. 2002). An alternative approach is to simply fit the data to Eq. 3 and then characterise the type of diffusion by the value of the coefficient α. Experimental values of $\alpha < 0.1$ may be considered as characteristic of confined diffusion (Fig. 5a): $0.9 < \alpha < 1.1$ indicates free diffusion (Fig. 5c); $0.1 < \alpha < 0.9$ is interpreted as obstructed diffusion (Fig. 5b); $\alpha > 1.1$ represents a directed motion (Fig. 5d). It should be noted that due to random variations even for the case of free diffusion, a value close to $\alpha = 1$ will only be obtained if a sufficiently high number of data points are averaged. For the movement of a free-diffusing particle, time periods can be selected from a single trajectory in which, due to random fluctuation, the particle moves with an apparent higher or lower MSD

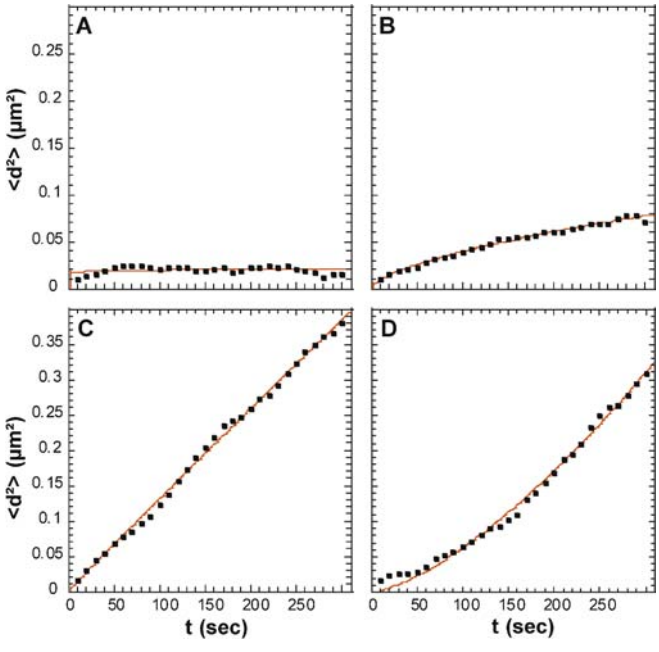

Fig. 5 According to the mean square displacement, four different types of mobility can be distinguished: **a** confined diffusion, **b** obstructed diffusion, **c** free diffusion and **d** directed motion. The *black squares* represent measured data using Mx1-YFP particles while the *red line* represents the fit according to Eq. 4

versus time. In order to distinguish these variations from the existence of distinct classes of particles, a histogram of the values of α or other parameters derived from SPT can be a useful diagnostic tool. If systematic deviations of the MSD data versus time are observed for a fit to Eq. 3, more complex descriptions have to be derived for a quantitative description of the particle mobility. Recently, we introduced the so-called "moving corral" (MC) model that describes the mobility of nuclear particles according to Eq. 4.

$$\mathrm{MSD} = \langle r_c^2 \rangle \left(1 + \frac{4D_c t}{\langle r_c^2 \rangle}\right)\left[1 - \exp\left(-\frac{4D_b t}{\langle r_c^2 \rangle}\right)\right] \qquad (4)$$

In the MC model, the overall mobility of the particle is described by a corral size of diameter r_c in which the particle experiences confined diffusion with a diffusion coefficient D_b. These chromatin corrals can then translocate according to a free diffusion model with a diffusion coefficient D_c. The derivation of this model has been described in detail previously (Görisch et al. 2004).

Chromatin dynamics

The diffusional properties of chromatin have been studied first by monitoring the mobility of a photobleached spot in dye-labelled chromatin (Abney et al. 1997). For individual tracking of subchromosomal regions, fluorescently labelled nucleotides were incorporated and diluted through subsequent segregation (Zink et al. 1998; Manders et al. 1999). The diffusion coefficients of 1.5×10^{-5} µm^2 s^{-1} for foci located on different territories and 5.0×10^{-6} µm^2 s^{-1} for foci located on the same territory were reported (Bornfleth et al. 1999).

As a technique to trace individual chromosome loci during interphase in living eukaryotic cells, the *lac* operator/LacI-GFP system was introduced by Belmont and co-workers (Robinett et al. 1996; Straight et al. 1996). It is based on the high-affinity binding of a bacterial lac-repressor protein fused with a GFP protein domain to multiple repeats of its recognition sequence stably integrated into the genome. Using the *lac*O/LacI-GFP system in mammalian cells as well as in yeast and Drosophila, rapid but locally restricted movements were found on a length scale of 0.4–0.5 µm (Marshall et al. 1997; Heun et al. 2001; Vazquez et al. 2001; Chubb et al. 2002). The movements of different sites in human living cells revealed that loci at nucleoli or the nuclear periphery are significantly less mobile than more nucleoplasmic loci. For the latter sites, a mean diffusion coefficient in human cells of 1.3×10^{-4} µm^2 s^{-1} was reported (Chubb et al. 2002). As an alternative approach to the lac-repressor system, peptide nuclei acid probes (PNAs) directed against specific sequences were also used to analyse the diffusional properties of chromatin (Molenaar et al. 2003). Using PNAs to analyse the diffusion of telomeres in human cells showed that the majority of telomeres

(~90%) revealed constrained diffusive movement (within confined nuclear regions of radius of ~230 nm) with a diffusion coefficient similar to that determined for nucleoplasmic lac arrays in human cells (Table 1).

Mobility of inert particles and nuclear bodies in the nucleus

The diffusion properties of inert nuclear particles, like beads or crystalline protein particles within the chromatin environment, were determined using SPT in a number of studies. Fluorescent nanospheres with a diameter of 100 nm microinjected into mouse 3T3 cells demonstrated nuclear movements, which were briefly restricted to a small cage or corral with an average diameter of 290 ± 50 nm. The MSD of the nanospheres in the nucleus showed a slight increase in time from 0 s to 0.1 s, an apparent plateau at 0.1–1 s (restricted motion within the corral) and a pronounced increase from 1 s to 10 s, which can be interpreted as escape of the nanosphere from the corral-type confinement (Tseng et al. 2004). Corralling was also observed using 100-nm polystyrene particles and NLS-vimentin bodies (Bacher et al. 2004). Crystalline nuclear particles (1.3 ± 0.06 μm) formed by murine Mx1-YFP showed a displacement of the particle centre within a corral with an average diameter of 600 nm (Fig. 6). We speculate that the regions accessible for these particles correspond to regions of lower chromatin density, as visualised by the weak staining with Hoechst 33258 shown in Fig. 6a, b. In addition, analysis of the Mx1-YFP particles indicated the presence of a slower component. This is assigned to movements of the surrounding chromatin leading to a translocation of the particles. Accordingly, movement of the Mx1-YFP particles could be accurately described by the MC model in which the nuclear bodies diffuse in and with a chromatin "corral" in the nucleus (Görisch et al. 2004).

Promyelocytic leukaemia and Cajal bodies displayed very similar average mobilities, as the biologically inert Mx1-YFP particles of similar size and their translocation in the nucleus could also be quantitatively described by the MC model (Görisch et al. 2004). This suggests that the body mobility reflects to a large extent the dynamics and accessibility of the surrounding chromatin environment. This view is supported by the observed co-localisation of nuclear bodies (discussed in Misteli 2001). In addition, chromatin regions around the nucleolus appeared to be devoid of nuclear bodies, consistent with the finding that the chromatin around the nucleolus is frequently more strongly condensed. In this context, it is also noteworthy that a significant fraction of mRNA molecules displayed corralled movements (Shav-Tal et al. 2004).

It has been shown that Cajal bodies are associated to several different snRNA and snoRNA gene loci as well as histone gene loci (Gall et al. 1981; Callan et al. 1991; Frey and Matera 1995; Schul et al. 1998; Jacobs et al. 1999). For PML bodies, an occasional association to the MHC gene region (Shiels et al. 2001), telomeres (Molenaar et al. 2003) and actively transcribed regions has been reported (Wang et al. 2004). These preferred localisations of nuclear bodies could be explained either by differences in the accessibility of nuclear regions and/or the binding to chromatin as it has been proposed for Cajal bodies (Platani et al. 2002). The analysis of a hamster cell line revealed that a fraction of PML bodies moved over longer distances in a directed and energy-dependent manner, suggesting that in this case also, active transport processes are involved. However, these faster-moving bodies were not observed in HeLa cells (Muratani et al. 2002; Görisch et al. 2004). The somewhat different interpretations with respect to the effect of energy depletion using sodium azide—increased Cajal body diffusion (Platani et al. 2002), decreased PML body (Muratani et al. 2002) and mRNP diffusion (Shav-Tal et al. 2004)—might indicate that multiple processes are effected. We and others observed that ATP depletion by treatment with sodium azide with or without deoxyglucose induced reversible chromatin condensation

Table 1 Corral size and diffusion coefficients of particles in the nucleus and chromatin loci

Particle/locus	r_c (nm)[a]	D (μm^2 s^{-1})	Reference
Mx1-YFP[b]	280	1.8×10^{-4}	Görisch et al. 2004
Cajal bodies[b]	310	1.1×10^{-4}	Görisch et al. 2004
PML bodies[b]	260	1.2×10^{-4}	Görisch et al. 2004
Nanospheres[c]	150	4×10^{-4}	Tseng et al. 2004
Nucleoplasmic chromatin[d]	240	1.3×10^{-4}	Chubb et al. 2002
Telomeres[e]	230	1.8×10^{-4}	Molenaar et al. 2003
Dense chromatin regions	180	4.8×10^{-5}	Görisch et al. 2004
1-Mb chromatin domain	–	$0.5–1.5\times10^{-5}$	Bornfleth et al. 1999

[a]The size of the region in which a given particle or the chromatin locus can translocate its centre of mass during an observation time of up to a few minutes is defined by a circle with radius r_c

[b]The given diffusion coefficient refers to the value D_c according to Eq. 4, which is believed to reflect the mobility of the chromatin environment

[c]The value of D was determined from MSD measurements at times from 3 s to 10 s

[d]A lacO array with integration site 5p14 was studied, which corresponds to a G band with a preferred localisation in the interior of the nucleoplasm

[e]Value observed for the majority of telomeres. A ~10% fraction of telomeres showed a higher mobility with a diffusion coefficient of $D = 5.8\times10^{-4}$ μm^2 s^{-1}

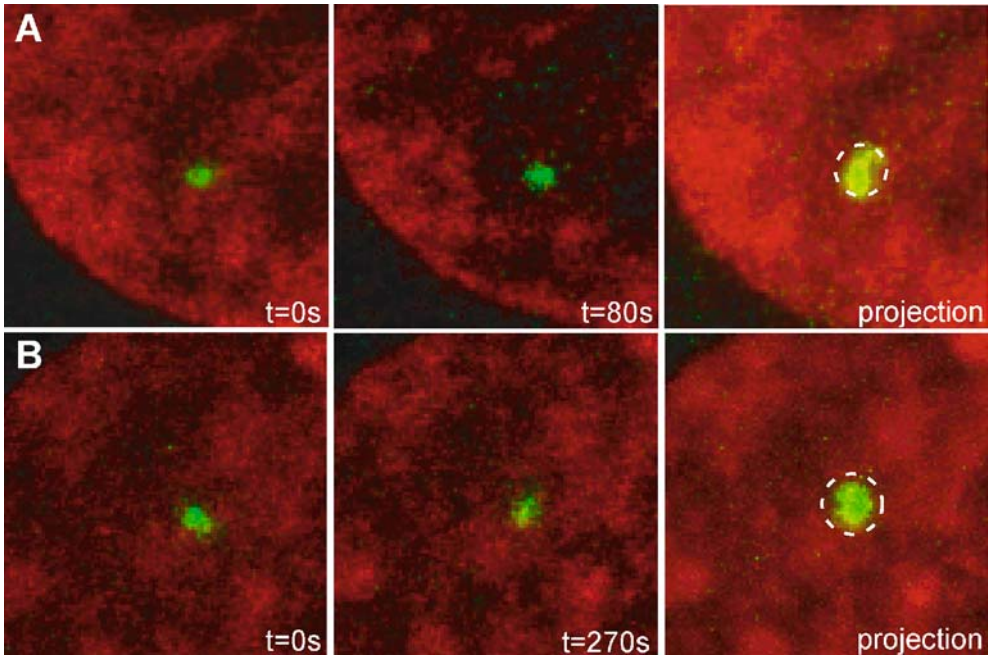

Fig. 6 Examples of corralled motion of nuclear particles. **a** and **b** show two different in vivo trajectories of an Mx1-YFP particle in a HeLa cell nucleus with Hoechst-33258-stained chromatin. The first and the last image of a time series taken over 80 s (**a**) and 270 s (**b**) and a maximum intensity projection of all images of the time series are shown. The expected average MSD determined from the trajectories of 100 Mx1-YFP particles (Görisch et al. 2004) is outlined by the *dashed white circle*. At short times (< 1 min), the centre of mass of the body displays relatively fast movements in a corral with a radius $r_c = 0.28 \pm 0.03$ μm. At longer observation times, a slow translocation of the region is observed in which the particle displays a corralled movement

(Görisch et al. 2004; Shav-Tal et al. 2004). This could also be related to the ATP-dependent activity of chromatin remodelling complexes (Corona and Tamkun 2004).

Model for nuclear body movement in the nucleus

In summary, the analysis of dextrans and nanospheres of a defined size indicates that the size-dependent accessibility, the confinement of the movement (''corralling'') and the dynamics of chromatin are important determinants for the mobility of large particles in the nucleus. Several conclusions can be arrived at:

The accessibility of chromatin for even very large protein complexes up to several MDa molecular weight (~20 nm in diameter) is essentially unrestricted within the resolution of the light microscope of ~250 nm. Particles of a size ≥30 nm, like 150 kDa and larger FITC dextrans, are progressively excluded from dense chromatin regions. This suggests that these bona fide heterochromatic regions have a dense chromatin fibre organisation with mesh sizes ≤ 30 nm in diameter, as discussed above. Larger particles with sizes around 100 nm (100-nm-diameter nanospheres, 2.5-MDa dextrans) are completely excluded from this chromatin mesh (Görisch et al. 2003; Tseng et al. 2004). This is certainly true also for the nuclear Cajal and PML bodies with a size of ~1 μm, which will therefore have access to only a subspace of the nucleus. Any movement of these bodies over distances above a few hundred nanometers will require a chromatin reorganisation that allows the separation of chromatin subdomains to create accessible regions within and through the chromatin network. The interface between chromosome territories (ICD) would provide such a subcompartment. This has been experimentally demonstrated for cells with distinctly different karyotypes by the above-mentioned ability of NLS-vimentin filaments to form between chromosome territories (Bridger et al. 1998; Reichenzeller et al. 2000; Scheuermann et al. 2005). In agreement with this model, a co-localisation of nuclear bodies and NLS vimentin in this ICD space has been observed (Zirbel et al. 1993; Bridger et al. 1998; Richter et al. 2005). Several experiments discussed above are summarised in Table 1 and indicate that the chromatin environment allows a random translocation of large particles in the nucleus by several hundred nanometers in the time scale of a few minutes or less. The movement can be described by a diffusion-type mobility of the particles' centre of mass in a corral with a radius of 200–300 nm (Table 1). This value is strikingly similar to the region in which the chromatin loci itself display a random movement. Furthermore, the chromatin locus mobility occurs with an apparent diffusion coefficient of up to $\sim 10^{-4}$ μm^2 s^{-1} (Chubb et al. 2002; Molenaar et al. 2003; Görisch et al. 2004), which is very similar to the diffusion coefficient calculated for the translocation of the chromatin corrals.

The experiments reviewed here, involving inert fluorescent macromolecules like dextrans or ectopically expressed proteins like NLS-vimentin filaments, as well as measurements of the mobility of nuclear bodies, nanospheres and chromatin loci, are included in the model presented in Fig. 7. As shown schematically on the left panel of Fig. 7, certain restrictions of the accessibility are imposed by the folding of the interphase chromatin fibre, as discussed above. The characteristics of the chromatin environment that define the mobility of PML and Cajal nuclear bodies are included in the MC model shown on the right side of Fig. 7. The size-

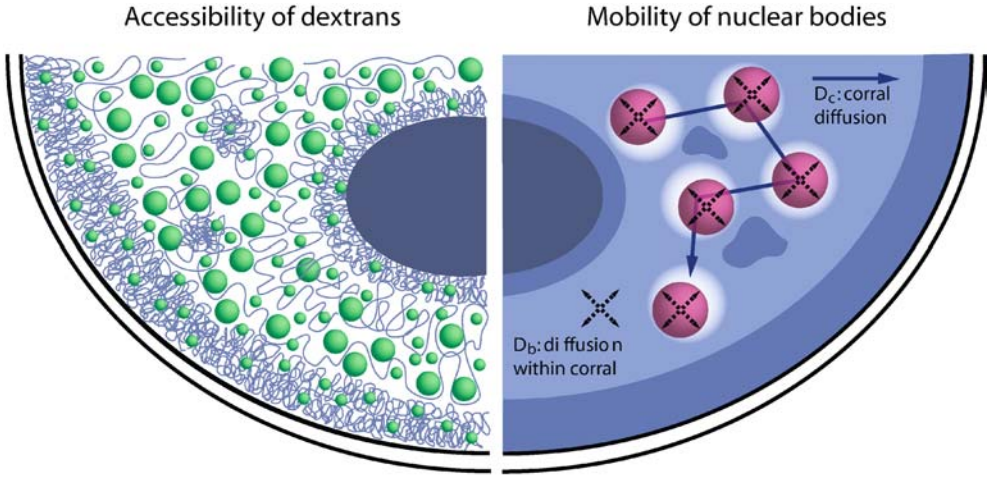

Fig. 7 Models for nuclear accessibility and body diffusion. The left image shows a section of a cell nucleus with macromolecules of different sizes that have, according to their sizes, unlimited nuclear access or are excluded from heterochromatic regions. The *right image* illustrates the moving corral model: nuclear bodies are enclosed in a chromatin "corral", which is defined by the chromatin accessibility. Within this accessible domain, they diffuse with the diffusion coefficient D_b while the chromatin corrals translocate within the nucleus with the diffusion coefficient D_c, as indicated by the *blue arrow*

dependent accessibility is reflected by the radius of the corral r_c, in which the body displays relatively fast movements with a diffusion coefficient D_b (Eq. 4). The movement of these corrals due to chromatin rearrangements is described by the diffusion coefficient D_c. This is obviously a simplification valid only for observation times in the order of several minutes since the maximal translocation of the corrals is limited by the finite size of the nucleus.

As discussed above, the nuclear subspace accessible for nuclear bodies is likely to include the interface between chromosome territories that allows a movement of the bodies by a transient separation of chromatin domains. By random movements, the nuclear bodies explore this accessible space and are expected to be localised more frequently in these more open chromatin regions. In as much as they coincide with regions of active gene transcription, they would also constitute possible biological targets of PML and Cajal bodies. This hypothesis can be tested by analysing the intranuclear mobility and localisation of multiple nuclear components simultaneously. With the availability of improved methods for imaging and data analysis in conjunction with new labelling techniques, it becomes possible to study nuclear bodies, RNA and chromatin loci in parallel within the same living cell and to identify their functional relations.

Acknowledgements We thank Stephanie Geiger for providing the image in Fig. 1a, Thibaud Jegou for helping with Fig. 7 and Katalin Fejes Tóth, Markus Scheuermann, Alessandro Brero, and Malte Wachsmuth for a critical reading of the manuscript as well as Harald Herrmann, Anje Sporbert, Karsten Richter and Ute Schmidt for fruitful discussions. Our work is supported by the Deutsche Forschungsgemeinschaft (grants Li 406/5-3, Ri 828/5-1) and the Volkswagen Foundation in the program Junior Research Groups at German Universities.

References

Abney JR, Cutler B, Fillbach ML, Axelrod D, Scalettar BA (1997) Chromatin dynamics in interphase nuclei and its implications for nuclear structure. J Cell Biol 137:1459–1468

Adkins NL, Watts M, Georgel PT (2004) To the 30-nm chromatin fiber and beyond. Biochim Biophys Acta 1677:12–23

Bacher CP, Reichenzeller M, Athale C, Herrmann H, Eils R (2004) 4-D single particle tracking of synthetic and proteinaceous microspheres reveals preferential movement of nuclear particles along chromatin—poor tracks. BMC Cell Biol 5:45

Bannister AJ, Zegerman P, Partridge JF, Miska EA, Thomas JO, Allshire RC, Kouzarides T (2001) Selective recognition of methylated lysine 9 on histone H3 by the HP1 chromo domain. Nature 410:120–124

Bastiaens PI, Pepperkok R (2000) Observing proteins in their natural habitat: the living cell. Trends Biochem Sci 25:631–637

Belmont AS, Bruce K (1994) Visualization of G1 chromosomes: a folded, twisted, supercoiled chromonema model of interphase chromatid structure. J Cell Biol 127:287–302

Berezney R, Dubey DD, Huberman JA (2000) Heterogeneity of eukaryotic replicons, replicon clusters, and replication foci. Chromosoma 108:471–484

Bornfleth H, Edelmann P, Zink D, Cremer T, Cremer C (1999) Quantitative motion analysis of subchromosomal foci in living cells using four-dimensional microscopy. Biophys J 77:2871–2886

Boyle S, Gilchrist S, Bridger JM, Mahy NL, Ellis JA, Bickmore WA (2001) The spatial organization of human chromosomes within the nuclei of normal and emerin-mutant cells. Hum Mol Genet 10:211–219

Braga J, Desterro JM, Carmo-Fonseca M (2004) Intracellular macromolecular mobility measured by fluorescence recovery after photobleaching with confocal laser scanning microscopes. Mol Biol Cell 15:4749–4760

Bridger JM, Herrmann H, Münkel C, Lichter P (1998) Identification of an interchromosomal compartment by polymerization of nuclear-targeted vimentin. J Cell Sci 111(Pt 9):1241–1253

Bridger JM, Kalla C, Wodrich H, Weitz S, King JA, Khazaie K, Kräusslich H-G, Lichter P (2005) Nuclear RNAs confined to a reticular compartment between chromosome territories. Exp Cell Res 302:180–193

Callan HG, Gall JG, Murphy C (1991) Histone genes are located at the sphere loci of Xenopus lampbrush chromosomes. Chromosoma 101:245–251

Chadwick BP, Willard HF (2003) Barring gene expression after XIST: maintaining facultative heterochromatin on the inactive X. Semin Cell Dev Biol 14:359–367

Chubb JR, Boyle S, Perry P, Bickmore WA (2002) Chromatin motion is constrained by association with nuclear compartments in human cells. Curr Biol 12:439–445

Corona DF, Tamkun JW (2004) Multiple roles for ISWI in transcription, chromosome organization and DNA replication. Biochim Biophys Acta 1677:113–119

Cremer M, von Hase J, Volm T, Brero A, Kreth G, Walter J, Fischer C, Solovei I, Cremer C, Cremer T (2001) Non-random radial higher-order chromatin arrangements in nuclei of diploid human cells. Chromosome Res 9:541–567

Cremer T, Cremer C, (2001) Chromosome territories, nuclear architecture and gene regulation in mammalian cells. Nat Rev Genet 2(4):292–301

Cremer T, Kupper K, Dietzel S, Fakan S (2004) Higher order chromatin architecture in the cell nucleus: on the way from structure to function. Biol Cell 96:555–567

Cremer T, Kurz A, Zirbel R, Dietzel S, Rinke B, Schrock E, Speicher MR, Mathieu U, Jauch A, Emmerich P, Scherthan H, Ried T, Cremer C, Lichter P (1993) Role of chromosome territories in the functional compartmentalization of the cell nucleus. Cold Spring Harb Symp Quant Biol 58:777–792

Croft JA, Bridger JM, Boyle S, Perry P, Teague P, Bickmore WA (1999) Differences in the localization and morphology of chromosomes in the human nucleus. J Cell Biol 145:1119–1131

Davies HG (1967) Fine structure of heterochromatin in certain cell nuclei. Nature 214:208–210

Dietzel S, Schiebel K, Little G, Edelmann P, Rappold GA, Eils R, Cremer C, Cremer T (1999) The 3D positioning of ANT2 and ANT3 genes within female X chromosome territories correlates with gene activity. Exp Cell Res 252(2):363–375

Dietzel S, Zolghadr K, Hepperger C, Belmont AS (2004) Differential large-scale chromatin compaction and intranuclear positioning of transcribed versus non-transcribed transgene arrays containing beta-globin regulatory sequences. J Cell Sci 117:4603–4614

Dillon N (2004) Heterochromatin structure and function. Biol Cell 96:631–637

Dillon N, Festenstein R (2002) Unravelling heterochromatin: competition between positive and negative factors regulates accessibility. Trends Genet 18:252–258

Durchschlag H (1986) Specific volumes of biological macromolecules and some other molecules of biological interest. In: Hinz H-J (ed) Thermodynamic data for biochemistry and biotechnology. Springer, Berlin Heidelberg New York, pp 45–128

Fejes Tóth K, Knoch TA, Wachsmuth M, Frank-Stöhr M, Stöhr M, Bacher CP, Müller G, Rippe K (2004) Trichostatin A-induced histone acetylation causes decondensation of interphase chromatin. J Cell Sci 117:4277–4287

Frey MR, Matera AG (1995) Coiled bodies contain U7 small nuclear RNA and associate with specific DNA sequences in interphase human cells. Proc Natl Acad Sci USA 92:5915–5919

Gall JG (2003) The centennial of the Cajal body. Nat Rev Mol Cell Biol 4:975–980

Gall JG, Stephenson EC, Erba HP, Diaz MO, Barsacchi-Pilone G (1981) Histone genes are located at the sphere loci of newt lampbrush chromosomes. Chromosoma 84:159–171

Görisch SM, Richter K, Scheuermann MO, Herrmann H, Lichter P (2003) Diffusion-limited compartmentalization of mammalian cell nuclei assessed by microinjected macromolecules. Exp Cell Res 289:282–294

Görisch SM, Wachsmuth M, Ittrich C, Bacher CP, Rippe K, Lichter P (2004) Nuclear body movement is determined by chromatin accessibility and dynamics. Proc Natl Acad Sci USA 101:13221–13226

Grewal SI, Rice JC (2004) Regulation of heterochromatin by histone methylation and small RNAs. Curr Opin Cell Biol 16:230–238

Hall LL, Lawrence JB (2003) The cell biology of a novel chromosomal RNA: chromosome painting by XIST/Xist RNA initiates a remodeling cascade. Semin Cell Dev Biol 14:369–378

Hamkalo BA, Rattner JB (1980) Folding up genes and chromosomes. Q Rev Biol 55:409–417

Hansen JC (2002) Conformational dynamics of the chromatin fiber in solution: determinants, mechanisms, and functions. Ann Rev Biophys Biomol Struct 31:361–392

Heitz R (1928) Das Heterochromatin der Moose. Jahrb Wiss Botanik 69:762818

Herrmann H, Lichter P (1999) New ways to look at the interchromosomal-domain compartment. Protoplasma 209:157–165

Heun P, Laroche T, Shimada K, Furrer P, Gasser SM (2001) Chromosome dynamics in the yeast interphase nucleus. Science 294:2181–2186

Jacobs EY, Frey MR, Wu W, Ingledue TC, Gebuhr TC, Gao L, Marzluff WF, Matera AG (1999) Coiled bodies preferentially associate with U4, U11, and U12 small nuclear RNA genes in interphase HeLa cells but not with U6 and U7 genes. Mol Biol Cell 10:1653–1663

Kimura H, Sugaya K, Cook PR (2002) The transcription cycle of RNA polymerase II in living cells. J Cell Biol 159:777–782

Kreth G, Finsterle J, von Hase J, Cremer M, Cremer C (2004) Radial arrangement of chromosome territories in human cell nuclei: a computer model approach based on gene density indicates a probabilistic global positioning code. Biophys J 86:2803–2812

Kurz A, Lampel S, Nickolenko JE, Bradl J, Benner A, Zirbel RM, Cremer T, Lichter P (1996) Active and inactive genes localize preferentially in the periphery of chromosome territories. J Cell Biol 135:1195–1205

Lachner M, O'Carroll D, Rea S, Mechtler K, Jenuwein T (2001) Methylation of histone H3 lysine 9 creates a binding site for HP1 proteins. Nature 410:116–120

Lamond AI, Sleeman JE (2003) Nuclear substructure and dynamics. Curr Biol 13:R825–R828

Lamond AI, Spector DL (2003) Nuclear speckles: a model for nuclear organelles. Nat Rev Mol Cell Biol 4:605–612

Lampel S, Bridger JM, Zirbel RM, Mathieu UR, Lichter P (1997) Nuclear RNA accumulations contain released transcripts and exhibit specific distributions with respect to Sm antigen foci. DNA Cell Biol 16:1133–1142

Lawrence JB, Singer RH, Marselle LM (1989) Highly localized tracks of specific transcripts within interphase nuclei visualized by in situ hybridization. Cell 57(3):493–502

Lénárt P, Rabut G, Daigle N, Hand AR, Terasaki M, Ellenberg J (2003) Nuclear envelope breakdown in starfish oocytes proceeds by partial NPC disassembly followed by a rapidly spreading fenestration of nuclear membranes. J Cell Biol 160:1055–1068

Lichter P, Cremer T, Borden J, Manuelidis L, Ward DC (1988) Delineation of individual human chromosomes in metaphase and interphase cells by in situ suppression hybridization using recombinant DNA libraries. Hum Genet 80:224–234

Lippincott-Schwartz J, Snapp E, Kenworthy A (2001) Studying protein dynamics in living cells. Nat Rev Mol Cell Biol 2:444–456

Lukacs GL, Haggie P, Seksek O, Lechardeur D, Freedman N, Verkman AS (2000) Size-dependent DNA mobility in cytoplasm and nucleus. J Biol Chem 275:1625–1629

Mahy NL, Perry PE, Bickmore WA (2002) Gene density and transcription influence the localization of chromatin outside of chromosome territories detectable by FISH. J Cell Biol 159:753–763

Maison C, Almouzni G (2004) HP1 and the dynamics of heterochromatin maintenance. Nat Rev Mol Cell Biol 5:296–304
Manders EM, Kimura H, Cook PR (1999) Direct imaging of DNA in living cells reveals the dynamics of chromosome formation. J Cell Biol 144:813–821
Marshall WF, Straight A, Marko JF, Swedlow J, Dernburg A, Belmont A, Murray AW, Agard DA, Sedat JW (1997) Interphase chromosomes undergo constrained diffusional motion in living cells. Curr Biol 7:930–939
Misteli T (2001) Protein dynamics: implications for nuclear architecture and gene expression. Science 291:843–847
Molenaar C, Wiesmeijer K, Verwoerd NP, Khazen S, Eils R, Tanke HJ, Dirks RW (2003) Visualizing telomere dynamics in living mammalian cells using PNA probes. Embo J 22:6631–6641
Müller WG, Rieder D, Kreth G, Cremer C, Trajanoski Z, McNally JG (2004) Generic features of tertiary chromatin structure as detected in natural chromosomes. Mol Cell Biol 24:9359–9370
Münkel C, Eils R, Dietzel S, Zink D, Mehring C, Wedemann G, Cremer T, Langowski J (1999) Compartmentalization of interphase chromosomes observed in simulation and experiment. J Mol Biol 285:1053–1065
Muratani M, Gerlich D, Janicki SM, Gebhard M, Eils R, Spector DL (2002) Metabolic-energy-dependent movement of PML bodies within the mammalian cell nucleus. Nat Cell Biol 4:106–110
Paul AL, Ferl RJ (1999) Higher-order chromatin structure: looping long molecules. Plant Mol Biol 41:713–720
Pienta KJ, Coffey DS (1984) A structural analysis of the role of the nuclear matrix and DNA loops in the organization of the nucleus and chromosome. J Cell Sci Suppl 1:123–135
Pinkel D, Landegent J, Collins C, Fuscoe J, Segraves R, Lucas J, Gray J (1988) Fluorescence in situ hybridization with human chromosome-specific libraries: detection of trisomy 21 and translocations of chromosome 4. Proc Natl Acad Sci USA 85:9138–9142
Platani M, Goldberg I, Lamond AI, Swedlow JR (2002) Cajal body dynamics and association with chromatin are ATP-dependent. Nat Cell Biol 4:502–508
Qian H, Sheetz MP, Elson EL (1991) Single particle tracking. Analysis of diffusion and flow in two-dimensional systems. Biophys J 60(4):910–921
Reichenzeller M, Burzlaff A, Lichter P, Herrmann H (2000) In vivo observation of a nuclear channel-like system: evidence for a distinct interchromosomal domain compartment in interphase cells. J Struct Biol 129:175–185
Richter K, Reichenzeller M, Görisch SM, Schmidt U, Scheuermann MO, Herrmann H, Lichter P (2005) Characterization of a nuclear compartment shared by nuclear bodies applying ectopic protein expression and correlative light and electron microscopy. Exp Cell Res 303:128–137
Rieger B, Molenaar C, Dirks RW, Van Vliet LJ (2004) Alignment of the cell nucleus from labeled proteins only for 4D in vivo imaging. Microsc Res Tech 64(2):142–150
Robinett CC, Straight A, Li G, Willhelm C, Sudlow G, Murray A, Belmont AS (1996) In vivo localization of DNA sequences and visualization of large-scale chromatin organization using lac operator/repressor recognition. J Cell Biol 135:1685–1700
Sachs RK, van den Engh G, Trask B, Yokota H, Hearst JE (1995) A random-walk/giant-loop model for interphase chromosomes. Proc Nat Acad Sci USA 92:2710–2714
Sako Y, Kusumi A (1994) Compartmentalized structure of the plasma membrane for receptor movements as revealed by a nanometer-level motion analysis. J Cell Biol 125:1251–1264
Saxton MJ (1994) Anomalous diffusion due to obstacles: a Monte Carlo study. Biophys J 66:394–401
Scheuermann MO, Tajbakhsh J, Kurz A, Saracoglu K, Eils R, Lichter P (2004) Topology of genes and nontranscribed sequences in human interphase nuclei. Exp Cell Res 301:266–279
Schul W, van Driel R, de Jong L (1998) Coiled bodies and U2 snRNA genes adjacent to coiled bodies are enriched in factors required for snRNA transcription. Mol Biol Cell 9:1025–1036
Sedat J, Manuelidis L (1978) A direct approach to the structure of eukaryotic chromosomes. Cold Spring Harb Symp Quant Biol 42 Pt 1:331–350
Seksek O, Biwersi J, and Verkman AS (1997) Translational diffusion of macromolecule-sized solutes in cytoplasm and nucleus. J Cell Biol 138:131–142
Shav-Tal Y, Darzacq X, Shenoy SM, Fusco D, Janicki SM, Spector DL, Singer RH (2004) Dynamics of single mRNPs in nuclei of living cells. Science 304:1797–1800
Shiels C, Islam SA, Vatcheva R, Sasieni P, Sternberg MJ, Freemont PS, Sheer D (2001) PML bodies associate specifically with the MHC gene cluster in interphase nuclei. J Cell Sci 114:3705–3716
Simson R, Yang B, Moore SE, Doherty P, Walsh FS, Jacobson KA (1998) Structural mosaicism on the submicron scale in the plasma membrane. Biophys J 74:297–308
Spector DL (2001) Nuclear domains. J Cell Sci 114:2891–2893
Spector DL (2003) The dynamics of chromosome organization and gene regulation. Annu Rev Biochem 72:573–608
Straight AF, Belmont AS, Robinett CC, Murray AW (1996) GFP tagging of budding yeast chromosomes reveals that protein–protein interactions can mediate sister chromatid cohesion. Curr Biol 6:1599–1608
Tanabe H, Muller S, Neusser M, von Hase J, Calcagno E, Cremer M, Solovei I, Cremer C, Cremer T (2002) Evolutionary conservation of chromosome territory arrangements in cell nuclei from higher primates. Proc Natl Acad Sci USA 99:4424–4429
Tseng Y, Lee JS, Kole TP, Jiang I, Wirtz D (2004) Micro-organization and visco-elasticity of the interphase nucleus revealed by particle nanotracking. J Cell Sci 117:2159–2167
Tumbar T, Sudlow G, Belmont AS (1999) Large-scale chromatin unfolding and remodeling induced by VP16 acidic activation domain. J Cell Biol 145:1341–1354
Vazquez J, Belmont AS, Sedat JW (2001) Multiple regimes of constrained chromosome motion are regulated in the interphase Drosophila nucleus. Curr Biol 11:1227–1239
Verschure PJ, van der Kraan I, Manders EM, Hoogstraten D, Houtsmuller AB, van Driel R (2003) Condensed chromatin domains in the mammalian nucleus are accessible to large macromolecules. EMBO Rep 4:861–866
Visser AE, Jaunin F, Fakan S, Aten JA (2000) High resolution analysis of interphase chromosome domains. J Cell Sci 113(Pt 14):2585–2593
Volpi EV, Chevret E, Jones T, Vatcheva R, Williamson J, Beck S, Campbell RD, Goldsworthy M, Powis SH, Ragoussis J, Trowsdale J, Sheer D (2000) Large-scale chromatin organization of the major histocompatibility complex and other regions of human chromosome 6 and its response to interferon in interphase nuclei. J Cell Sci 113(Pt 9):1565–1576
Wachsmuth M, Waldeck W, Langowski J (2000) Anomalous diffusion of fluorescent probes inside living cell nuclei investigated by spatially-resolved fluorescence correlation spectroscopy. J Mol Biol 298:677–689
Wang J, Shiels C, Sasieni P, Wu PJ, Islam SA, Freemont PS, Sheer D (2004) Promyelocytic leukemia nuclear bodies associate with transcriptionally active genomic regions. J Cell Biol 164:515–526
Weidemann T, Wachsmuth M, Knoch TA, Müller G, Waldeck W, Langowski J (2003) Counting nucleosomes in living cells with a combination of fluorescence correlation spectroscopy and confocal imaging. J Mol Biol 334:229–240
Woodcock CL, Dimitrov S (2001) Higher-order structure of chromatin and chromosomes. Curr Opin Genet Develop 11:130–135
Xing Y, Johnson CV, Dobner PR, Lawrence JB (1993) Higher level organization of individual gene transcription and RNA splicing. Science 259:1326–1330
Zink D, Bornfleth H, Visser A, Cremer C, Cremer T (1999) Organization of early and late replicating DNA in human chromosome territories. Exp Cell Res 247(1):176–188

Zink D, Cremer T, Saffrich R, Fischer R, Trendelenburg MF, Ansorge W, Stelzer EH (1998) Structure and dynamics of human interphase chromosome territories in vivo. Hum Genet 102:241–251

Zirbel RM, Mathieu UR, Kurz A, Cremer T, Lichter P (1993) Evidence for a nuclear compartment of transcription and splicing located at chromosome domain boundaries. Chromosome Res 1:93–106